

AIAA 81-0726R

# Interaction between the RIT 10 Exhaust and Negatively Charged Surfaces

K.H. Groh,\* K. Bescherer,† N.K. Nikolaizig,† and H.W. Loeb‡  
*University of Giessen, Federal Republic of Germany*

Spacecraft charging in geosynchronous orbit up to several kilovolts by electrons from the plasma environment is a well-known hazard to the satellite. To study these phenomena, a substorm facility has been built at Giessen University by modifying a 28 m<sup>3</sup> vacuum chamber. The main goal of the work is to study the behavior of different materials under electron irradiation and the interaction between the RIT 10 electric propulsion system and the charged surfaces. Preliminary tests have demonstrated that it is possible to compensate for the negative charge with ions from the thruster and/or the plasma bridge neutralizer.

## Introduction

SATELLITES exposed to the plasma environment at high altitudes accumulate a charge from the plasma electrons in the same way as probes immersed in a plasma. The spacecraft potential with respect to the ambient plasma depends on the satellite's outer surface materials and their conductivity as well as on the plasma environment. Extremely high potentials up to -10 to -20 kV are obtained in the local midnight-to-dawn period associated with geomagnetic substorm activities.<sup>1-3</sup>

Coincident with this, anomalous behavior of geosynchronous spacecraft has been observed, such as control circuit switching, power system failure, sensor data noise, and telemetry logic switching. This behavior must be attributed to the spacecraft charging effects or more likely to the discharges taking place between adjacent surfaces that have accumulated different electrostatic charges. In situ measurements by the ATS-5 and ATS-6 satellites and lately by the SCATHA satellite have more or less confirmed the assumed correlations between anomalous behavior and spacecraft charging and have provided inputs to the theoretical models of spacecraft charging phenomena.

Moreover, onboard particle sources have allowed the evaluation of these satellites' response to the ejection of ions or electrons. Experiments have demonstrated the ability to clamp the potential of a satellite by emitting electrons.<sup>4,5</sup> These facts were known (except SCATHA) when in 1979 ground tests were started to study the possibility of controlling spacecraft charging via the RIT 10 electric propulsion system. The experiments were performed in the large vacuum facility of Giessen, P 100,000, which had been built for ion thruster testing.

The following sections outline the modifications necessary to build a substorm facility with electron irradiation and diagnostic equipment. The different materials used for the thermal blanketing or coating of the satellite surface were irradiated under substorm conditions and monitored for their response. The results are reported here, along with a description of the operation of the RIT 10 electric propulsion system close to the charged surfaces.

## The Test Facility

The P 100,000 test facility,<sup>6</sup> a horizontal cylinder 5.30 m in length and 2.70 m in diameter, is very well suited as a substorm facility since it is large enough to allow the installation of the scanning device and diagnostic tools described below. Two frames bear the samples which can be alternately turned into the electron beam. This mechanism has the advantage of testing two different samples without venting the chamber to the atmosphere. The two oil diffusion pumps with a 100,000 l/s pumping speed provide a vacuum in the low 10<sup>-6</sup> Torr region that is necessary to avoid interaction with the residual gas (the mean free path is about 10 m).

The chamber itself and all components are manufactured of nonmagnetic stainless steel. (The Earth's magnetic field of about 0.3 G is present but not intensified by the metal parts and does not cause a large deflection of the electron beam.) Windows at the top, bottom, and sides of the chamber allow visual inspection and photographic documentation of the irradiated samples.

The electron gun is mounted outside the main chamber separated by a valve and is thus accessible at any time. Further details about the gun and the characteristics of the electron beam are given in a following section on irradiation of samples.

The basic test setup is shown in Fig. 1. On the left side is the electron gun and in the middle of the chamber are the diagnostic tools explained in the next section.

## Diagnostic Equipment

The diagnostic instruments determine the parameters of the electron beam such as electron density and energy, the surface potential of the irradiated sample, the current in the groundline from the sample, and arc discharges (if occurring). The schematic diagram shown in Fig. 2 demonstrates the test setup. It is divided into three sections: the generation of the electron beam, the diagnostic of the beam, and the examination of the samples.

Since the electron beam is produced via a scattering foil, an energy analyzer is necessary in addition to the current density sensor. The electron energy sensor is of the electrostatic type. Through an entrance slit, the electrons penetrate the electrical field of a cylindrical capacitor with two bent electrodes. The geometry of the analyzer has been calculated so that the voltage applied to the electrodes of the capacitor corresponds to the energy of the incident electrons.

Electrons with corresponding energy pass the velocity separating field and enter a Faraday cup where they are detected. The analyzer is laid out for an energy range of 0-30 keV and has an accuracy within 5%.

Presented as Paper 81-0726 at the AIAA/JSASS/DGLR 15th International Electric Propulsion Conference, Las Vegas, Nev., April 21-23, 1981; submitted April 29, 1981; revision received Oct. 2, 1981. Copyright © American Institute of Aeronautics and Astronautics, Inc., 1981. All rights reserved.

\*Head of Electric Propulsion Working Group, 1st Institute of Physics.

†Research Scientist, 1st Institute of Physics.

‡Head of the Department, 1st Institute of Physics.

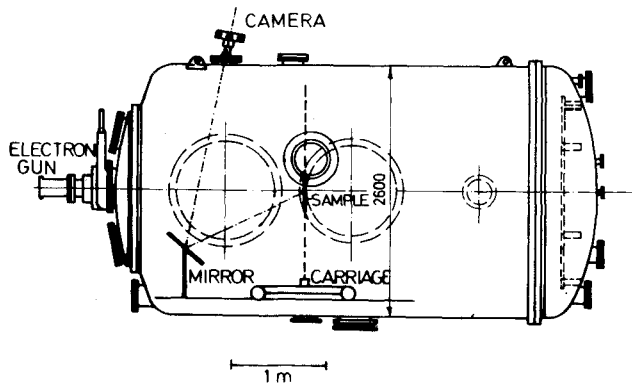


Fig. 1 Cross section of the substorm facility.

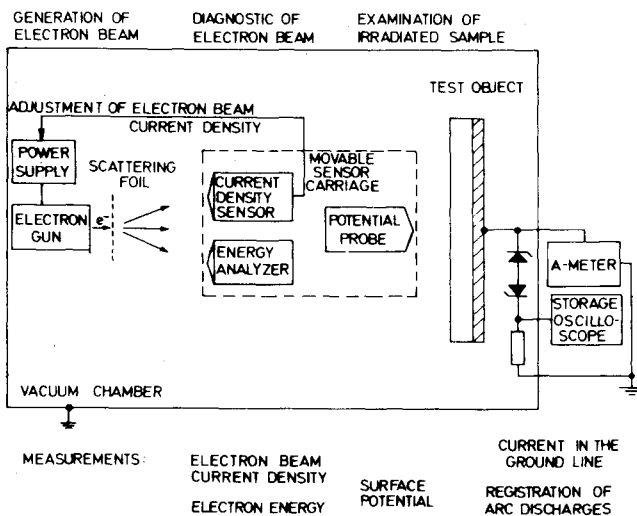


Fig. 2 Diagnostic equipment and setup for measuring.

The electron density must be monitored during irradiation of the samples. This is done by a  $100 \text{ cm}^2$  aluminum plate which is grooved in order to suppress secondary electrons. The density sensor is mounted on the scanning device, allowing determination of the beam parameters across the entire cross section of the produced electron beam. To meet the requirement of uniformity in the beam of better than 20% for a  $40 \times 40 \text{ cm}$  sample, the electron density is checked before each test.

The most important criterion for the experiments is the surface potential of the samples. This potential can be measured only by a noncontacting method. Moreover, potentials up to  $-20 \text{ kV}$  are possible and, if present, will have to be measured with a surface resolution of better than  $100 \text{ cm}^2$ .

For these reasons, a noncontacting electrostatic voltmeter, the TREK-type 340 HV, was chosen. This voltmeter is equipped with a miniature probe which can be operated in a high vacuum. The small probe surface ( $1 \text{ cm}^2$ ) guarantees excellent resolution. Due to the measurement method of the TREK voltmeter, the probe  $V$  is adjusted to the same potential as the unknown of the sample. In this manner, the potential distribution on the samples is not disturbed by the measurement equipment. However, referring to the floating probe, a good insulation of the probe mounting support, the cable, and the vacuum feed-through is indispensable for proper operation. The slew rate of the voltmeter is greater than  $0.4 \text{ V}/\mu\text{s}$ , which avoids any sparking between the probe and the sample. Nevertheless, the measuring of potentials above  $15 \text{ kV}$  repeatedly led to interruptions in the experiments because of breakdowns in the voltmeter itself between the

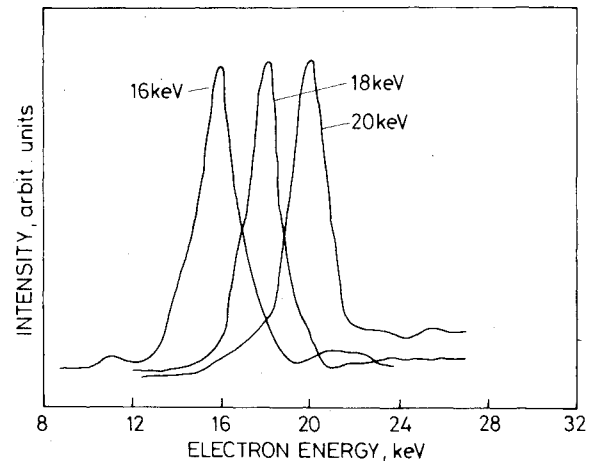


Fig. 3 Energy distribution of the scattered electron beam.

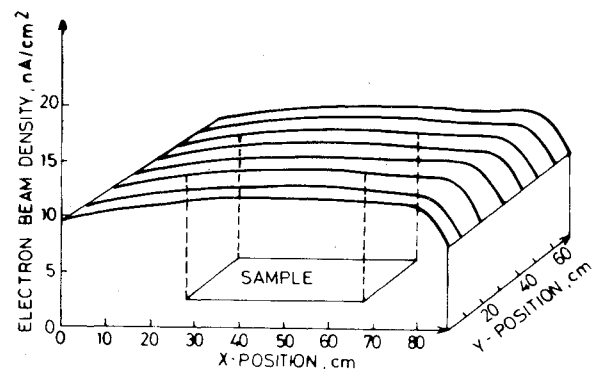


Fig. 4 Electron density profile for irradiation of the samples.

high-voltage floating parts and the grounded parts. These problems finally caused a severe delay in the time schedule of the experiments, which is the reason that only preliminary results are presently available on these tests of the influence of the RIT 10 motor on charged samples.

Beside the scanning device with the diagnostic equipment, the RIT 10 ion motor is mounted with the plasma bridge neutralizer on the top of the thruster case. The ion engine is swivel-mounted allowing canting angles from firing parallel to the sample to  $90^\circ$  away from the sample. In this way, the influence of the canting angle between the ion engine and the charged sample can be studied.

### Irradiation of Samples

The experiments were divided into two major phases: the electron irradiation of the samples and the tests with the RIT 10 on the irradiated samples. Prior to irradiation of the samples the characteristic of the electron beam had to be determined as described below.

The purpose of the electron gun was to simulate substorm conditions. This required a current density of  $1\text{--}10 \text{ nA}/\text{cm}^2$  at an electron energy of up to  $20 \text{ keV}$ . Moreover, a uniformity of 20% over the sample area was demanded. This was not possible with a simple electron gun and it was decided to use a gun combined with a scattering foil. That is, the accelerated electrons were scattered at a  $0.75 \mu\text{m}$  thick aluminum foil which smoothed the beam profile so that the required uniformity was obtained.<sup>7</sup> However, due to the energy absorption of the foil, the electrons were not monoenergetic but had an energy distribution and, due to the fact that current absorption depends on the energy, there existed a lower energy limit of about  $14 \text{ keV}$  which restricted the use of this method. Furthermore, care had to be taken to illuminate the scattering foil uniformly to avoid melting it. Figure 3 shows

the energy distribution of the scattered electrons of the three energy levels used for irradiation.

The uniformity achieved by this method is 8% over the sample surface of  $40 \times 40$  cm and about 24% over the total area of  $80 \times 80$  cm it was possible to scan in these tests. Figure 4 shows the electron density as a function of the position of the current density sensor. For illustration the sample area is depicted.

Under these conditions, the samples irradiated were of 2, 3, 5, and 10 mil metallized Teflon which is used on satellites as a second-surface mirror. The tests were carried out in two steps: 1) the irradiation of the samples and 2) the discharge of the samples. Prior to each irradiation, the electron beam parameters were checked to be sure that they met the proper test conditions.

During the irradiation, the parameters measured were: 1) the surface potential as a function of the position and the irradiation time; and 2) the current from the metallic backside of the sample to the ground. During the discharge of the sample (electron gun switched off), the parameters measured were: 1) the surface potential as a function of the discharge time; and 2) the current from the ground to the metallic backside. Since the surface potential distribution was uniform across the sample, the potential has scanned only in the  $X$  direction at a fixed  $Y$  position.

If arc discharges occurred (valid for the 2 and 3 mil Teflon samples), the total surface was scanned to obtain data about the potential distribution.

How are the currents that flow during the charging and discharging of the samples to be explained? During irradiation, an electron current flows from the metallic substrate to the ground consisting of the charging current and the leakage current through the dielectric. At equilibrium, only the leakage current contributes to the measured current.

After switching off the electron gun, the current reverses its polarity: electrons flow from the ground to the sample. This current, three orders of magnitude smaller than the charging current, can be explained by electrons leaving the sample into the vacuum by field or photoemission mechanisms.

Two of the examined samples (2 and 3 mil Teflon) showed arc discharges. Arc discharges give a response in the groundline if the charge leaves the sample surface. Charges transferred to the substrate directly through the dielectric or along the dielectric surface cancel with their image charge and do not contribute to the current in the groundline.

In the following paragraphs, some representative results will be given characterizing the sample's response to the irradiation. Figure 5 demonstrates the increase of the surface potential for the four mentioned Teflon samples under 20 keV irradiation. With increasing thickness of the Teflon sheath, the leakage current becomes smaller and steady-state con-

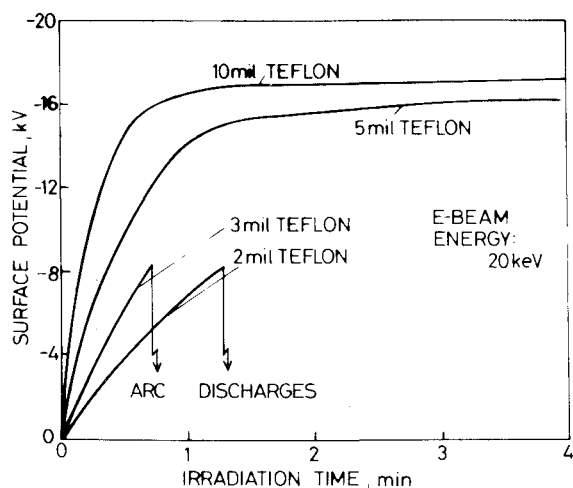


Fig. 5 Potential of different samples for 20 keV beam energy.

ditions are obtained earlier. On the 2 and 3 mil samples, arc discharges occurred at about 8 kV surface potential.

The charging currents are plotted in Fig. 6. The left side of the curves represents the charging of the samples. The linear part of the curves in the equilibrium case is caused by the leakage current of the dielectric which depends on the applied field strength and increases with increasing beam energy.

A typical surface potential profile after a discharge is shown in Fig. 7 for a 3 mil sample. The sample was scanned horizontally only in the middle of the surface. Scans were performed in time steps of 6 s until breakdown occurred. It can be seen that only parts of the surface are discharged and other parts retain their charge. This means that differential charging is caused not only by different materials, but also on a homogeneous surface after arc discharges have taken place.

The results for lower electron beam energies or lower beam current densities do not differ in principle from those shown above. Lower energies result in correspondingly lower steady-state potentials and lower irradiation densities cause longer irradiation times to obtain the same potential.

### Tests of RIT 10 on Irradiated Samples

Due to the problems with the electrostatic voltmeter described above, the experiments with the RIT 10 have just started. In this paper only preliminary tests can be reported and the influence on the samples discussed.

For these experiments, a RIT 10 of the prototype level was equipped with a plasma bridge neutralizer. A detailed

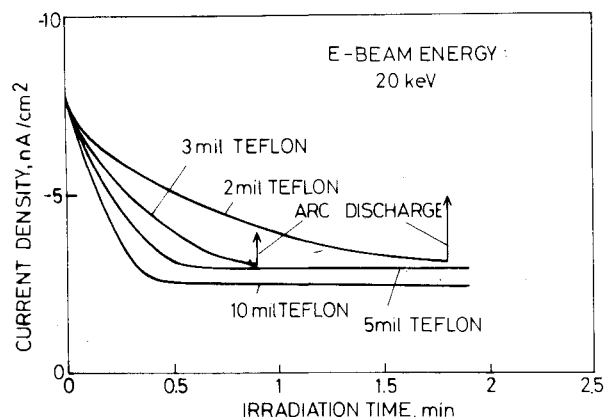


Fig. 6 Charging current for different samples.

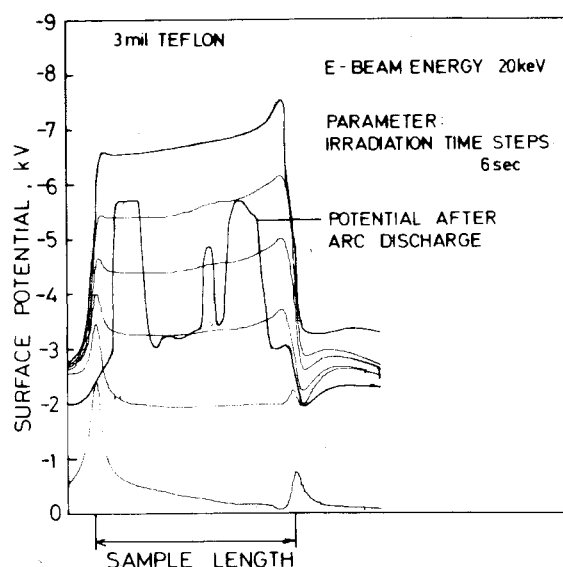


Fig. 7 Potential growth and decay after arc discharge for a 3 mil Teflon sample.

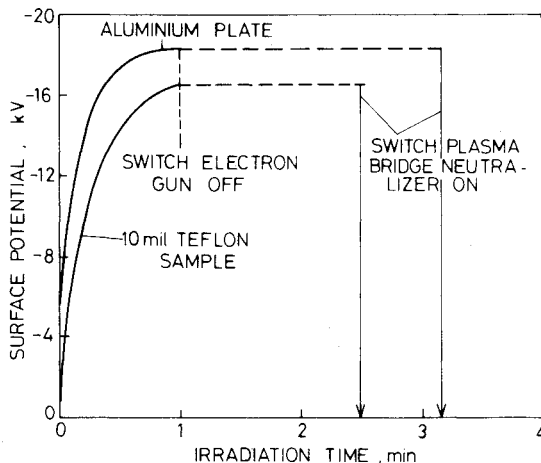


Fig. 8 Potential drop of the samples by firing the plasma bridge neutralizer of the RIT 10.

description of the engine and the neutralizer is given in Refs. 8 and 9. The ion motor and electron source are supplied by a power conditioning unit which allows automatic as well as hand operation. For the reported tests it is important to operate the ion source and/or the electron source separately in order to distinguish between the effects of the thrusters, ion exhaust and the effects caused by the neutralizer electrons or its small plasma cloud of the dc discharge.

For these tests, a 10 mil Teflon sample and a pure metallic aluminum plate were chosen. At first, the samples were charged to about 18 kV surface potential. Starting the mercury discharge of the plasma bridge neutralizer it was found that the surface potential dropped immediately to a few volts when the discharge was ignited. This behavior was found at the aluminum plate as well as at the Teflon sample. That means a coupling exists between the charged sample and the plasma cloud of the neutralizer sufficient to compensate the negative charge on the samples. These tests have been repeated for different angles between the sample and the neutralizer; but even when firing the neutralizer looking away from the sample, a decrease of the surface potential was found.

Replacing the aluminum plate by the 10 mil Teflon sample we found hints of an influence of the distance between the sample and the plasma source. Figure 8 shows two potential curves for both samples demonstrating the effect of firing the neutralizer and the dropping of the potential.

Simulating the other case where a satellite with a working plasma source enters a substorm, the plasma bridge neutralizer was started first and then an attempt was made to charge the samples. But for both samples, no clear increase of the potential due to the electron irradiation could be found. This means that it makes no difference whether the plasma source is operated before or after the sample has charged. The potential can be clamped down in both cases.

## Conclusion

The first experiments to check the influence of the RIT 10 exhaust on irradiated samples showed that already the small plasma cloud of the plasma bridge neutralizer is able to compensate the negative charge of the sample and to clamp the surface potential to the 100 V range. Of course, similar results are obtained firing the ion engine itself. This means that an electric propulsion system on board a satellite can be used not only for propulsion purposes, but much more as a tool to control the satellite potential. Even the differential charging of surfaces can be avoided.

## Acknowledgments

The reported experiments are part of the Doctorate Theses of the coauthors K. Beschere and N. Nikolaizig.

The work is sponsored by the European Space Agency ESA/ESTEC under Contract 3639/78/NL/AK which is gratefully acknowledged.

## References

- <sup>1</sup>De Forest, S.E., "Spacecraft Charging at Synchronous Orbit," *Journal of Geophysical Research*, Vol. 77, Feb. 1972, p. 651.
- <sup>2</sup>Rosen, A., "Large Discharges and Arc on Spacecraft," *Astronautics & Aeronautics*, Vol. 13, June 1975, p. 36.
- <sup>3</sup>Inouye, G.T., "Spacecraft Charging Model," AIAA Paper 75-255, 1975.
- <sup>4</sup>Goldstein, R., "Active Control of Potential of the Geosynchronous Satellites ATS-5 and ATS-6," AFGL-TR-77-0051/NASA TMX-73537, 1977.
- <sup>5</sup>De Forest, S.E., "Electrostatic Potentials Developed by ATS-5," *Photon and Particle Interactions with Surfaces in Space*, edited by G. Grard, Dodrecht, Boston, 1973, p. 263.
- <sup>6</sup>Klein, W., Groh, K., and Lang, H., "Optimization of the Rf-Thruster RIT 20," AIAA Paper 72-474, 1972.
- <sup>7</sup>Feibig, W., Görler, G., and Klein, G., "Electron Irradiation Experiments on Two Types of Surface Blankets of the Satellite OTS," DFVLR-RS Final Report IB 353-77/14, 1977.
- <sup>8</sup>Loeb, H. et al., "Recent Tests of the RIT 10 Engine at Giessen University," AIAA Paper 76-1037, 1976.
- <sup>9</sup>Groh, K. et al., "Recent Neutralizer Investigations at Giessen University," AIAA Paper 76-989, 1976.